POLITECNICO DI TORINO
Repository ISTITUZIONALE

Optimization of irregular-shaped resonant plates for pyroshock testing in the aerospace industry

Original
Optimization of irregular-shaped resonant plates for pyroshock testing in the aerospace industry / Viale, L., Daga, A.P., Fasana, A., Garibaldi, L.. - ELETTRONICO. - (2024), pp. 730-738. (31st International Conference on Noise and Vibration Engineering, ISMA 2024 Leuven (BEL) 9 - 11 September 2024).

Availability:
This version is available at: 11583/2998024 since: 2025-03-03T15:49:41Z

Publisher:
KU Leuven, Departement Werktuigkunde

Published
DOI:

Terms of use:

This article is made available under terms and conditions as specified in the corresponding bibliographic description in the repository

Publisher copyright

(Article begins on next page)

25 November 2026

Optimization of irregular-shaped resonant plates for pyroshock testing in the aerospace industry

L. Viale, A.P. Daga, A. Fasana, L. Garibaldi
Politecnico di Torino, Department of Mechanical and Aerospace Engineering,
Corso Duca degli Abruzzi 24, 10129, Torino, Italy
e-mail: **luca.viale@polito.it**

Abstract
The simulation of pyroshock tests through resonant plates is a standard procedure to verify the resistance of space equipment to high-frequency shocks generated by pyrotechnic devices. These shocks lead to significant risks, potentially compromising missions. Space qualification criteria – typically expressed in Shock Response Spectrum (SRS) terms – vary based on launch vehicle characteristics and follow the guidelines provided in international standards such as the NASA-STD-7003A. This study employs a frequency domain-based numerical model and a heuristic optimization algorithm to optimize resonant plate designs, considering irregular quadrilateral shapes. Integrating a CAD modeler, finite element solver, and genetic algorithm optimizer improves SRS prediction accuracy, reduces calibration times, and minimizes trial-and-error repetitions. While adopted decisions may influence specific outcomes, this work outlines a general methodology applicable across diverse requirements and constraints.

1 Introduction

In the aerospace and defense industries, pyrotechnic devices utilizing high-energy or explosive materials are essential for performing key mechanical operations such as the separation of spacecraft stages, cargo satellites, boosters, structural subsystems, and the deployment of various components. The activation of these explosive charges generates a transient mechanical response in nearby structural elements, particularly near the energy release point. This phenomenon, known as pyrotechnic shock or pyroshock, is characterized by its impulsive nature and high-frequency response. Pyroshocks frequently damage electronic components and occasionally cause structural failures, potentially compromising space missions.

To ensure the reliability and functionality of aerospace and defense equipment, international standards require the manufacturers of space and aerospace equipment to test the instruments' ability to withstand the strong excitations produced during launch. Specifically, to verify the mechanical resilience of space and aerospace equipment to pyroshocks, manufacturers must adhere to experimental protocols outlined in standards, such as NASA 7003 [1] and ESA ECSS [2]. These standards generally specify a Shock Response Spectrum (SRS) as the testing criterion. The SRS represents the frequency content of shocks and is commonly used to assess their potential for damage [3], [4]. Typically, the maxi-max SRS, which indicates the absolute maximum response in terms of acceleration, is employed. This measurement is conducted using a standardized array of mass-spring-damper systems, each with a Single Degree Of Freedom (SDOF). These systems are tuned to natural frequencies to achieve a frequency resolution of 1/24 octave, with a damping coefficient of $\zeta_{SRS} = 0.05$.

The most effective and widely used technique for emulating pyroshock effects in a controlled and safe environment exploits resonant plates as resonant fixtures [5], [6]. In this testing method, the test object is attached to one side of a large metal plate. The other side of the plate is struck by an impactor, such as a dropping mass, pendulum, projectile, hammer, or piston. An anvil plate may be strategically positioned at the impact site to control the impulse duration and magnitude, as illustrated in Figure 1. The impact energy

excites the plate, which generates a pyroshock response. Despite being the standard requirement, the SRS is not so intuitive, as many different combinations of testing parameters can produce similar curves [7]. As a result, researchers have studied the effect of various test parameters on the pyroshock response [8], [9]. These parameters include the plate's boundary conditions, the material and geometry of the impactor, the impact velocity and location, and the anvil plate material. Additionally, numerical models have been developed to simulate pyroshock tests and optimize testing parameters.

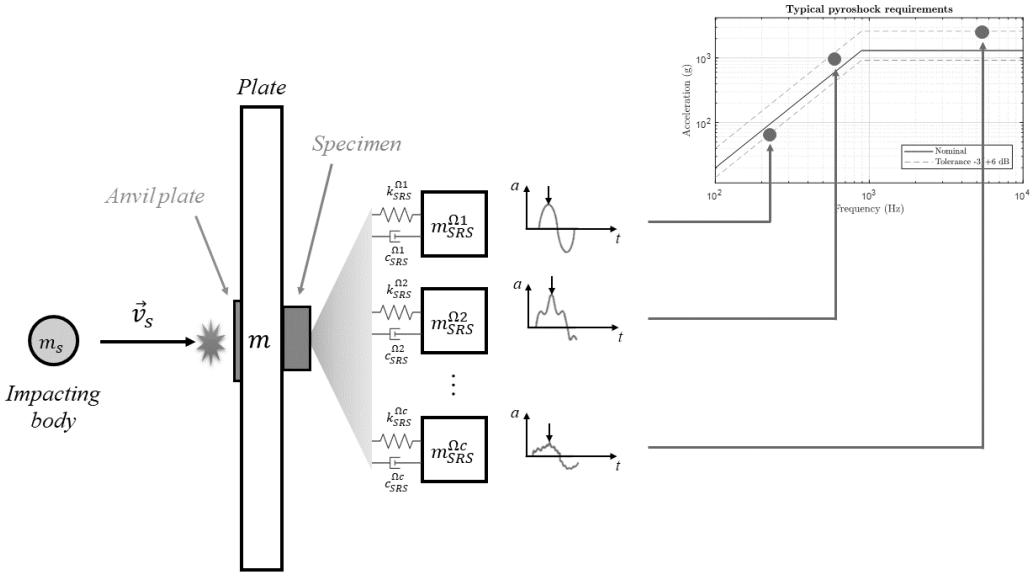

Figure 1. Schematic representation of a pyroshock test facility and SRS computation diagram.

Existing numerical models for simulating pyroshock tests are too complex and computationally expensive to be used to automate the selection of test parameters. To address this limitation, the works presented in [10], [11] have proposed a simpler numerical model based on a simplified Multi-Degree Of Freedom (MDOF) model with lumped masses and stiffnesses, and a frequency domain convolutional scheme. This simplified model allows a quick and reliable tuning of all the main test variables.

Nevertheless, the proposed work exploits a numerical model for pyroshock testing based on a Finite Element Model (FEM) [12]. The FE model is more advanced than the previously used MDOF model, and it provides more accurate results at the cost of slightly longer computational times. However, the time cost remains manageable because the contact simulation is not included in the FE model. The exploited numerical model can be used to perform a novel heuristic optimization of the shape and size of a resonant plate in order to faithfully match the simulated and the required SRS. This research focuses on shape and size optimization among irregular quadrilateral shapes. Due to the significant influence of various parameters and the complexity of their interactions, comprehensive parameter exploration can substantially reduce test calibration times and provide significant economic benefits by eliminating costly trial-and-error procedures.

The present paper is structured as follows. Section 2 briefly introduces the exploited frequency domain model, and the complete description of the model to optimize the resonant plate shape and size. Finally, Section 3 and 4 report the optimized results and conclusions, respectively.

2 Methodology

2.1 Numerical Simulation Model

The proposed approach exploits a reasonably fast and accurate model for simulating the SRS generated by a shock due to the impact of a projectile on a base plate. The frequency domain model reported in [12] is based on the physical model shown in Figure 1. For the sake of simplicity, it could be decomposed into three sub-models as outlined in Figure 2:

- A finite element model of a resonant plate with an anvil and a test object mounted in variable points of the surface that can compute the point inertance of a metal plate of any shape and material. The geometry of the resonant plate, along with the anvil plate and the specimen, can be parametrically defined by the CAD software, which is OpenSCAD [13]. This CAD tool facilitates the generation of complex geometries while preserving parametric flexibility.
- A numerical model for the impact, which defines the input pulse signal according to the principles of the contact mechanics (as a function of the contact materials and projectile momentum). The definition of the force-time pulse curve is established by three main characteristics: the impact duration, the coefficient of restitution and the function describing the curve, which depend on the properties of the impacting bodies.
- A numerical model for computing the maximax SRS with a Q factor of 10, i.e., the maximum of the absolute value of the time acceleration of a hypothetical Single Degree Of Freedom (SDOF) mass mounted on the plate with a damping factor of 5%. The SDOF mass is iterated over a range of natural frequencies (typically from 100 to 10.000 Hz) to cover the entire frequency range of interest.

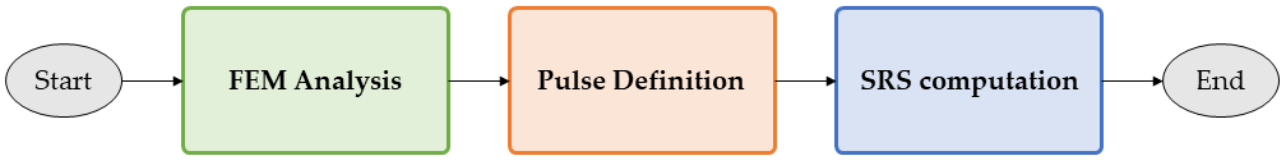

Figure 2. Simplified block diagram of the exploited numerical model described in [12].

The three sub-models are then merged using a frequency domain convolutional scheme to speed up the procedure. To reach the definition of these three sub-models, the mathematical steps governing the computation of SRS acceleration, incorporating known parameters and addressing both the direct and inverse problems, are briefly summarized in the following equation, where the SRS acceleration $\ddot{X}_{SRS}(\omega)$ has been decomposed into the following product:

$$\ddot{X}_{SRS}(\omega) = F(\omega) \cdot \frac{X(\omega)}{F(\omega)} \cdot \frac{X_{SRS}(\omega)}{X(\omega)} \cdot \frac{\ddot{X}_{SRS}(\omega)}{X_{SRS}(\omega)} \tag{1}$$

where $F(\omega)$ is the spectrum of the applied pulse, $X(\omega)$ is the displacement of the plate, $X_{SRS}(\omega)$ is the displacement of the SRS mass, $\ddot{X}_{SRS}(\omega)$ its acceleration, and ω is the frequency. It can be observed that the ratios composing the product represent well-known physical quantities, such as specific frequency response functions. Indeed, $\frac{X(\omega)}{F(\omega)}$ is precisely the definition of receptance. Eq. (1) can be reformulated as:

$$\ddot{X}_{SRS}(\omega) = \underbrace{\Delta p_s \cdot F^*(\omega)}_{Pulse\ definition} \cdot \underbrace{\alpha(\omega)}_{Plate\ dynamics} \cdot \underbrace{-\omega^2 \cdot T(\omega)}_{SRS\ computation} \tag{2}$$

where $F^*(\omega)$ is the spectrum of a pulse with unitary momentum (the force value mainly depends on the duration τ of the pulse), $\alpha(\omega)$ is the receptance obtained considering the specific location of the input force and the output measurement, Δp_s is the momentum demanded to reach the level of the SRS requirements, and $T(\omega)$ is the transmissibility of each SRS system.

2.2 Test Facility Optimization

In the literature, there is no standard for conducting pyroshock tests. Indeed, one can observe a large number of test benches with different configurations, excitation systems, and resonant devices. The resonant plates themselves often vary in terms of geometry, dimensions, material, orientation, and boundary conditions. Typically, the definition of these experimental setups is based on empirical techniques, technician's past experience, and results obtained through trial and error. Most test facilities for shock tests in the literature use a square or rectangular resonant plate. For instance, [9] and [14] use square aluminum alloy plates with dimensions of $1 \times 1 \times 0.03$ m^3 and $1 \times 1 \times 0.05$ m^3, respectively. Instead, [15] analyzes a rectangular plate with dimensions of $1.2 \times 0.5 \times 0.03$ m^3.

Given that the proposed frequency model accurately predicts the SRS under varying operating conditions with high accuracy and flexibility, this work aims to optimize some of its numerous parameters in order to fill some literature lacks. The focus is on geometric parameters, exploiting a reverse engineering process. In fact, the optimal combination of shapes and dimensions of a resonant plate are studied to meet canonical requirements.

In the simulation model, the geometric parameters are typically fixed, as the plate geometry does not vary, and the goal is to determine the appropriate momentum to meet the shock test requirements. However, the model can be extended to solve the inverse problem, i.e., optimizing the resonant plate for given requirements.

This work investigates how the shape and size of the resonant plate affect the SRS profiles. A genetic algorithm is used to search for the optimal plate. The implementation of an embedded CAD modeler and a FE solver allows the prediction of the behavior of a resonant plate with a complex and variable shape.

In addition to the geometry of the resonant plate, the mass m_s and velocity v_s of the impacting object are also optimized, as the mass of the plate is proportional to its size. More massive plates require higher momentum and vice versa. This allows for the optimization of the SRS profile independent of other confounding factors. All parameters have been discretized in specific ranges to avoid local minima problems, which are typical of heuristic optimizers.

Finally, a score function must be defined to solve the minimization problem. Among the most commonly used evaluation criteria are the Root Mean Square Error (RMSE) and the Mean Absolute Error (MAE). However, the score function has been determined specifically for this case. Since pyroshock requirements are typically established with associated tolerances, the score function is adapted to evaluate the error only when the SRS falls outside the tolerance region. Additionally, the score function should consider the fact that undertesting conditions are more critical than overtesting conditions. For all these reasons, the score function adopted in this work is defined as:

$$score_{GA} = \begin{cases} \dfrac{\log_{10}(\ddot{X}_{SRS}) - \log_{10}(\ddot{X}_r)}{\log_{10}(\ddot{X}_{tol}^{+}) - \log_{10}(\ddot{X}_r)} - 1 & if \quad \ddot{X}_{SRS} > \ddot{X}_{tol}^{+} \\ 0 & if \quad \ddot{X}_{tol}^{-} \leq \ddot{X}_{SRS} \leq \ddot{X}_{tol}^{+} \\ \dfrac{\log_{10}(\ddot{X}_{SRS}) - \log_{10}(\ddot{X}_r)}{\log_{10}(\ddot{X}_{tol}^{-}) - \log_{10}(\ddot{X}_r)} - 1 & if \quad \ddot{X}_{SRS} < \ddot{X}_{tol}^{-} \end{cases} \tag{3}$$

where $\ddot{X}_{SRS}(\Omega_c)$ is the calculated value of the acceleration synchronized to the resonant frequency Ω_c of the c-th SDOF system for the SRS calculation, $\ddot{X}_r(\Omega_c)$ is the test requirement (or the generic reference curve) in terms of SRS acceleration, $\ddot{X}_{tol}^{-}$ and $\ddot{X}_{tol}^{+}$ are respectively the values of the lower and upper tolerances. For the sake of clarity, Figure 3 shows the colormap representing the score applied to the SRS predictions, considering a standard requirement.

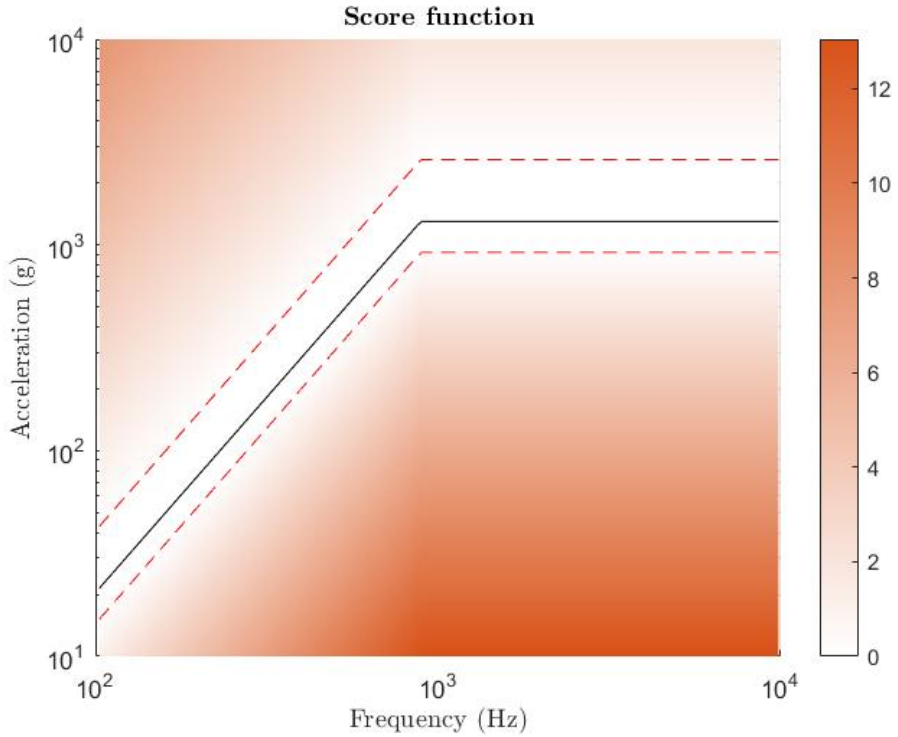

Figure 3: Colormap describing the adopted score function according to the specified requirements and the related tolerances.

This analysis was developed to investigate whether there may exist resonant plates with irregular shapes that satisfy the requirements better than regular polygonal plates, commonly used for pyroshock tests in the literature. Since the analysis of any irregular shape would be excessively extensive, the investigation has been limited to irregular quadrilateral shapes. These geometries generate a notable range of configurations and limit the overall population at the same time, as well as the parameters to be optimized.

The flexibility of the simulation model used allows the definition of the irregular quadrilateral plates by fixing the coordinates $(x_V; y_V)$ of its vertices $V = 1,2,3,4$, as shown in Figure 4. To avoid any redundancies due to the symmetries of the geometry, one of the vertices has been fixed (V_1 coincides with the origin of the reference system). The remaining vertices were limited to established regions of space. The definition of these regions defines also the maximum and minimum dimensions of the plate ($2 \times 1 \times 0.05$ m^3 and $1 \times 0.5 \times 0.01$ m^3 respectively). In addition, their definition makes it possible to consider irregular triangular shapes since they correspond to degenerate quadrilateral cases. The Table 1 shows the parameters

optimized by GA and their established discretization. In addition to the coordinates of the vertices, GA also optimizes the thickness z_p of the plate, the mass m_s, and the velocity v_s of the impacting object, considering that the mass of the plate is proportional to its size. Indeed, as previously mentioned, larger plates necessitate higher momentum, and vice versa. This approach improves the optimization of the SRS profile, making it independent of other potential confounding factors. To mitigate the risk of encountering local minima, typical of heuristic optimizers, all parameters are discretized within specific ranges.

Table 1. Discretization of the parameters optimized by GA for the irregular quadrilateral case.

Parameter	Lower Bound	Discretization	Upper Bound
x_2	0 m	0.1 m	0.5 m
y_2	1 m	0.1 m	2 m
x_3	0.5 m	0.1 m	1 m
y_3	1 m	0.1 m	2 m
x_4	0.5 m	0.1 m	1 m
y_4	0 m	0.1 m	1 m
z_p	0.01 m	0.01 m	0.05 m
m_s	1 kg	2 kg	9 kg
v_s	1 m/s	2 m/s	9 m/s

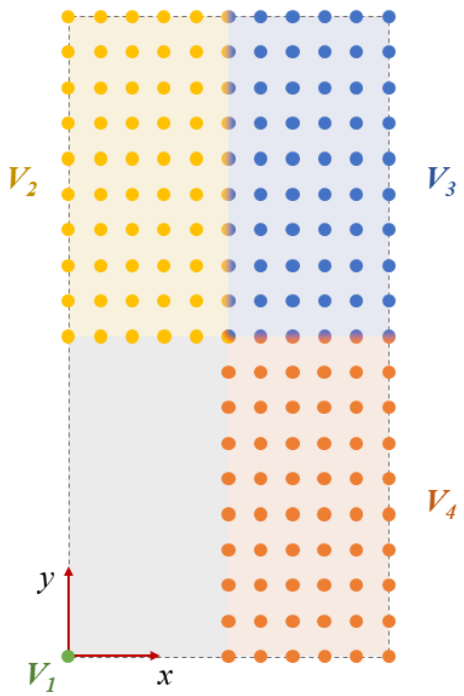

Figure 4: Diagram of the discretization grid outlining parameters for optimizing the irregular geometry of the resonant plate.

The other parameters were set, including the plate material (in the specific case, an aluminum alloy), the impact and measurement points (both established in the center of gravity of the plate). Since the multivariate space generated by the parameters to be optimized contains a higher number of possible combinations, a population size of 200 was chosen to initialize the genetic algorithm, considered the best trade-off between the density of analyzed cases in the multidimensional space and calculation times. Additionally, to ensure

algorithm convergence while minimizing runtime, the number of iterations was set to 10. The score function that regulates the optimization is reported in Eq. (3) and shown in Figure 3.

3 Results and Discussion

The GA-optimized irregular quadrilateral plate has been obtained as previously described, and the resulting geometry is shown in Figure 3, while Table 2 shows the optimized parameters adopted in the simulation. It can be observed that the resulting shape is rather complex and difficult to extract using other methodologies. The geometry of this plate can be motivated through the principles of wave propagation. At the same time, the specific imposed conditions may influence the result and lead to this precise geometry.

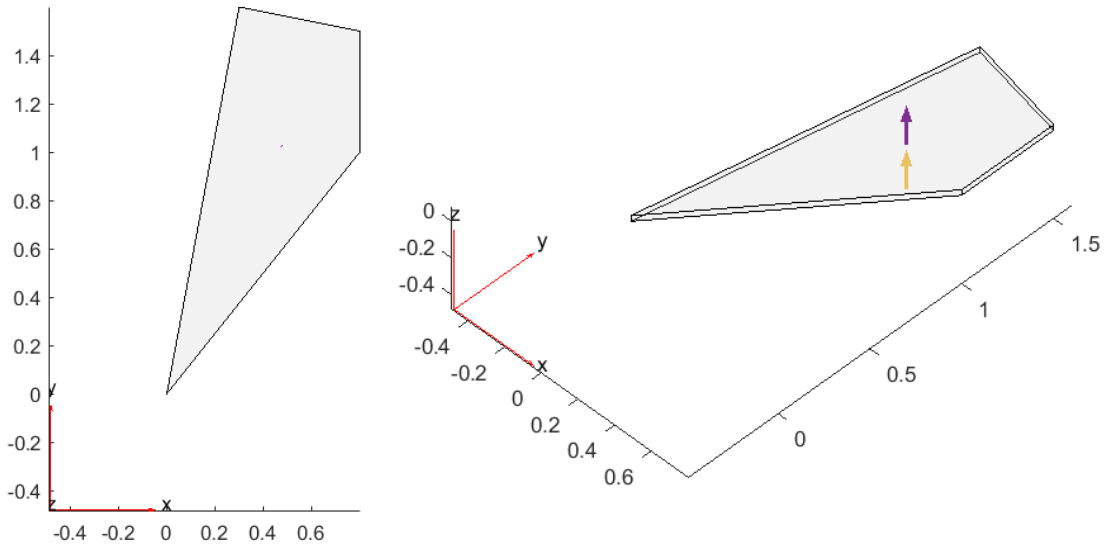

Figure 5. Resulting optimization of the irregular quadrilateral shaped and sized resonant plate.

Table 2: Fixed and optimized (indicated by the superscript *) parameters adopted to simulate the optimal configuration with the irregular shape.

Parameter	Value
V_1	(0 m; 0 m)
V_2*	(0.3 m; 1.6 m)
V_3*	(0.8 m; 1.5 m)
V_4*	(0.8 m; 1 m)
z_p*	0.03 m
m_s*	9 kg
v_s*	1 m/s
Plate material	Al6082
Impact location	Center of mass (0.475 m; 1.025 m)
Measurement location	Center of mass (0.475 m; 1.025 m)
Boundary conditions	Free
Impacting object material	SS303
Impacting object curvature	0.2 m
Force profile shape	von Hann window

Figure 6 shows the simulated SRS with the new optimized plate. It is worth noting how the curve falls perfectly within the tolerance ranges, flawlessly satisfying the imposed requirements. It cannot be excluded

that other equivalent solutions exist within the population of considered plates (i.e., plates with irregular quadrilateral geometry and dimensions within the set range).

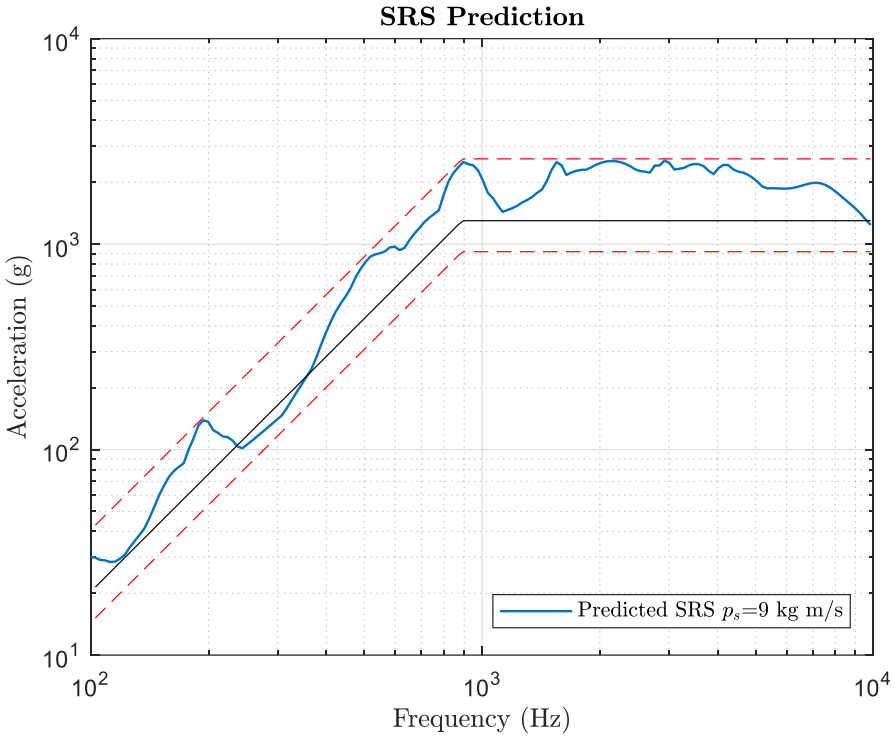

Figure 6. Simulated SRS inherent to the GA-optimized resonant plate with the trapezoidal scalene shape.

4 Conclusions

The focus of this study was on optimizing a pyroshock test facility from a geometric perspective. The research utilized a numerical model capable of fully simulating a pyroshock test, integrating an embedded CAD modeler and a FE solver. The flexibility and accuracy of this model enabled a GA optimization of the shape and size of a resonant plate to match the required SRS.

The optimization process explored various irregular quadrilateral shapes to investigate more complex geometries. This analysis resulted in a resonant plate that enhanced the predicted SRS, remaining within specified tolerance ranges. This improvement can be attributed to wave propagation within the plate and its vibration modes under the specific test conditions.

Given the complexity of pyroshock test facilities and the significant influence of their parameters and interactions on the resulting SRS, this study demonstrated enhanced accuracy in SRS prediction. More importantly, it contributed to substantial reductions in calibration times during the tuning process and avoided costly trial-and-error iterations.

In conclusion, it is acknowledged that specific configurations were considered in this analysis, and the outcomes may vary based on the decisions made. Nonetheless, this work aimed to outline a general methodology applicable to diverse requirements and constraints.

References

[1] H. Himelblau, “Pyroshock Test Criteria,” NASA-STD-7003A, 2011.

[2] E. S. A. ECSSSecretariat and R. ESTEC, “ECSS-E-ST-10-03C,” *Space Engineering-Testing, ESA Publications Division, Noordwijk, The Netherlands*, no. 2, 2012.

[3] A. Calvi *et al.*, “ECSS-E-HB-32-26A Spacecraft Mechanical Loads Analysis Handbook,” *undefined*, 2013.

[4] C. M. Harris and A. G. Piersol, *Harris’ shock and vibration handbook*, vol. 5. McGraw-Hill New York, 2002.

[5] Y. Yan and Q. M. Li, “A pyroshock signal characterization method based on shock-waveform dictionary,” *International Journal of Mechanical Sciences*, vol. 249, p. 108251, 2023.

[6] J.-R. Lee, C. C. Chia, and C.-W. Kong, “Review of pyroshock wave measurement and simulation for space systems,” *Measurement*, vol. 45, no. 4, pp. 631–642, May 2012, doi: 10.1016/j.measurement.2011.12.011.

[7] C. Sisemore, “Defining Resonant Plate Shock Test Specifications in the Time Domain.,” Sandia National Lab.(SNL-NM), Albuquerque, NM (United States), 2019.

[8] C. Sisemore and M. A. Spletzer, “Design of a Resonant Plate Shock Fixture to Attenuate Excessive High-Frequency Energy Inputs.,” Sandia National Lab.(SNL-NM), Albuquerque, NM (United States), 2017.

[9] M. Jonsson, “Development of a shock test facility for qualification of space equipment,” *Department of Applied Mechanics, Göteborg, Sweden*, 2012.

[10] L. Viale, A. P. Daga, L. Garibaldi, and A. Fasana, “Numerical Modeling of a Pyroshock Test Plate for Qualification of Space Equipment,” in *European Workshop on Structural Health Monitoring*, P. Rizzo and A. Milazzo, Eds., in Lecture Notes in Civil Engineering. Cham: Springer International Publishing, 2023, pp. 990–999. doi: 10.1007/978-3-031-07322-9_100.

[11] A. P. Daga, L. Viale, L. Garibaldi, A. Fasana, and S. Marchesiello, “Frequency domain convolutional model of a pyroshock plate for qualification of space equipment,” *AIP Conference Proceedings*, vol. 2872, no. 1, p. 120011, Sep. 2023, doi: 10.1063/5.0164212.

[12] L. Viale, A. P. Daga, A. Fasana, and L. Garibaldi, “On pyroshock tests for aerospace equipment qualification: A comprehensive parametric model for the simulation and the design of pyroshock test facilities,” *International Journal of Impact Engineering*, vol. 180, p. 104697, Oct. 2023, doi: 10.1016/j.ijimpeng.2023.104697.

[13] “OpenSCAD.” Accessed: Jul. 22, 2022. [Online]. Available: https://openscad.org

[14] B.-S. Kim and J. Lee, “Development of Impact Test Device for Pyroshock Simulation Using Impact Analysis,” *Aerospace*, vol. 9, no. 8, p. 407, 2022.

[15] O. M. F. Morais and C. M. A. Vasques, “Shock environment design for space equipment testing,” *Proceedings of the Institution of Mechanical Engineers, Part G: Journal of Aerospace Engineering*, vol. 231, no. 6, pp. 1154–1167, 2017.